

Stability of the chain structure in liquid K_xTe_{1-x} ($x=0.0, 0.2,$ and 0.5): *Ab initio* molecular-dynamics simulations

Fuyuki Shimojo and Kozo Hoshino

Faculty of Integrated Arts and Sciences, Hiroshima University, Higashi-Hiroshima 739-8521, Japan

Y. Zempo

Sumitomo Chemical, 6 Kitahara, Tsukuba 300-3294, Japan

(Received 5 July 2000; revised manuscript received 16 October 2000; published 12 February 2001)

The stability of local chain structures formed by Te atoms in liquid K_xTe_{1-x} mixtures ($x=0.0, 0.2,$ and 0.5) is studied by *ab initio* molecular-dynamics simulations. It is confirmed by investigating the atomic and electronic structures that at $x=0.2$, the chain structure of Te is stabilized by the presence of K atoms compared with the pure liquid Te, and that, at the equiatomic concentration, most of the Te atoms form the Te_2^{2-} dimers, as expected by the Zintl rule. From the time evolution of local atomic configurations, it is found that the Zintl Te_2^{2-} dimers interact with each other, and the bond breaking and the rearrangement of dimers occur rather frequently.

DOI: 10.1103/PhysRevB.63.094206

PACS number(s): 61.25.Mv, 71.22.+i, 71.15.Pd

I. INTRODUCTION

Liquid Te exhibits metallic properties with an electrical conductivity of about $2000 (\Omega \text{ cm})^{-1}$ near the melting point, while its solid phase is a typical semiconductor. It has been experimentally known¹⁻³ that the electrical conductivity decreases monotonically with the addition of alkali elements; at 50% of alkali concentration, it is only about $1 (\Omega \text{ cm})^{-1}$. Both experimental⁴⁻⁶ and theoretical⁷ studies have suggested that this metal-semiconductor transition in the liquid alkali tellurides is closely related to the change in the chain structure of Te atoms by adding alkali elements.

The neutron-diffraction experiments^{4,6} for liquid K_xTe_{1-x} and Rb_xTe_{1-x} mixtures showed the persistence of covalently bonded Te atoms in the liquids. For lower alkali concentrations $x \leq 0.2$, the measured structures are similar to that of the pure liquid Te. However, the separation of the first peak of the pair distribution function from the rest of neighbors becomes clear when alkali elements are added, and the Te-Te coordination number decreases with increasing alkali concentration. In the case of the equiatomic mixture $K_{0.5}Te_{0.5}$, the measured structure shows a virtually complete pairing of Te atoms that are identified with Zintl ions Te_2^{2-} .

Recently, *ab initio* molecular-dynamics (MD) simulations⁷ were carried out for liquid Rb_xTe_{1-x} mixtures ($x=0.0, 0.2,$ and 0.5). It was shown that the interchain interactions are suppressed by Rb^+ ions, and therefore the Te chains are relatively stabilized in comparison with the pure liquid Te. For $x=0.5$, more than half of Te atoms form Te_2^{2-} dimers, which are mixed with short Te chains and Rb^+ ions. These results are consistent with the experimental observations. It was also shown by calculating the partial density of states that almost complete charge transfer from Rb to Te occurs in the mixtures. The spatial distribution of the transferred charge in the Te chains was investigated. The structure of liquid K_xTe_{1-x} mixtures was also investigated by *ab initio* MD simulations.⁸ It was reported that Te dimers are formed in the equiatomic $K_{0.5}Te_{0.5}$ mixture.

It is, therefore, undoubted that the Te chains are stabilized by adding alkali elements so as to reduce the number of threefold-bonded defects⁴ that are believed to be contained in pure liquid Te and are responsible for the metallic conduction, and that there exist the Zintl ions Te_2^{2-} at the equiatomic concentration. These facts explain the decrease in the electrical conductivity with increasing alkali elements. However, there have been no quantitative discussions about the stability of the Te chain in liquid alkali tellurides. Especially, it is interesting to investigate the stability of the Zintl ions Te_2^{2-} in the liquids. In the structure of crystalline alkali-Te compounds at the equiatomic concentration,^{2,9} all Te atoms exist as Te_2^{2-} dimers, being consistent with the Zintl rule,^{10,11} which suggests the presence of Te_2^{2-} dimers if a complete charge transfer from the alkali atom to Te occurs. Since the results of the *ab initio* MD simulations⁷ showed that the charge transfer is almost complete in the liquid alkali tellurides, there is an indication that the Te_2^{2-} anions are also stable in the liquids. However, in the snapshots of the atomic configuration obtained by the MD simulations, there exist short chains that consist of more than two Te atoms and isolated Te atoms, as well as the Te_2^{2-} dimers. It is, therefore, worthwhile investigating the stability of the Zintl anions.

To study the stability of polyanions predicted by the Zintl rule,^{10,11} several *ab initio* MD simulations have been carried out for liquid mixtures, such as KSi ,¹² $NaSn$,¹³ $LiPb$,¹⁴ $NaPb$,¹⁵ KPb ,¹⁶ $CsPb$,¹⁷ and KSb .¹⁸ In the liquid mixtures of group IV elements with alkali metals, the Zintl anions are supposed to have tetrahedral complexes. In the liquid K-Sb (group V element) mixture, chainlike polyanions are considered to be present. However, no theoretical study for investigating the stability of Zintl anions in the liquid alkali group VI element mixtures has been reported so far.

In this paper, we present the results of our *ab initio* MD simulations for investigating the dynamic properties of the Te chain structure in liquid alkali tellurides, especially the stability of the Zintl ions Te_2^{2-} . In the liquid alkali-Te mix-

tures, only for K-Te mixtures the neutron-diffraction measurements were carried out for higher alkali concentrations (up to 50%). Therefore, we have chosen to calculate the properties of liquid K_xTe_{1-x} mixtures so as to compare the calculated structures with the experimental results.

In Sec. II, the method of *ab initio* MD simulations used here is briefly described. The results of our simulation and discussions are given in Sec. III. Finally we summarize our work in Sec. IV.

II. METHOD OF CALCULATION

Our calculations were performed within the framework of the density-functional theory, in which the generalized gradient approximation¹⁹ was used for the exchange-correlation energy. The electronic wave functions were expanded in the plane-wave (PW) basis set. The energy functional was minimized using an iterative scheme based on the preconditioned conjugate-gradient method.^{20–22} For the interaction between the valence electrons and ions, we used the ultrasoft pseudopotentials^{23,24} obtained from the electronic structure calculations for $K(3p^63d^04s^1)$ and $Te(5s^25p^45d^0)$ atoms.

The cubic supercell contains 80 atoms and the periodic boundary conditions were imposed. The simulations were carried out at three K concentrations; K_xTe_{1-x} with $x = 0.0, 0.2,$ and 0.5 . The temperatures and densities are (750 K, 0.0272 \AA^{-3}), (710 K, 0.0244 \AA^{-3}), and (710 K, 0.0196 \AA^{-3}) for $x = 0.0, 0.2,$ and 0.5 , respectively. Using the Nosé-Hoover thermostat technique,^{25,26} the equations of motion were solved via the velocity Verlet algorithm with a time step $\Delta t = 2.4 \times 10^{-15}$ s. The Γ point was used for the Brillouin-zone sampling, and the PW cutoff energies for the wave functions and the charge density are 10 and 65 Ry, respectively, which are chosen so as to give a good convergence of the total energy. The quantities of interest are obtained by averaging over about 5 ps after the initial equilibration taking about 2 ps.

III. RESULTS

A. Atomic structure

In various kinds of partial structure factors to characterize the structure of a binary mixture, we employ the Ashcroft-Langreth formulas,²⁷ which are defined as

$$S_{\alpha\beta}(k) = (N_\alpha N_\beta)^{-1/2} \left[\left\langle \sum_{i=1}^{N_\alpha} \sum_{j=1}^{N_\beta} \exp\{-ik \cdot (\mathbf{r}_{\alpha i} - \mathbf{r}_{\beta j})\} \right\rangle - (N_\alpha N_\beta)^{1/2} \delta_{k,0} \right], \quad (1)$$

where N_α is the total number of α -type atoms, and $\mathbf{r}_{\alpha i}$ is the position of i th α -type atom. The $S_{\alpha\beta}(k)$ for $x = 0.2$ and 0.5 are shown in Figs. 1(a) and 1(b), respectively. The $S_{TeTe}(k)$ has a peak at about $k = 1.1 \text{ \AA}^{-1}$, which becomes higher with increasing K concentration. In the $S_{KK}(k)$, the corresponding peak is recognized for $x = 0.2 \text{ \AA}^{-1}$. For $x = 0.5$, this peak becomes broad, and a dip appears at about $k = 2.5 \text{ \AA}^{-1}$. The $S_{KTe}(k)$ has a negative dip at about $k = 1.1 \text{ \AA}^{-1}$, a first peak

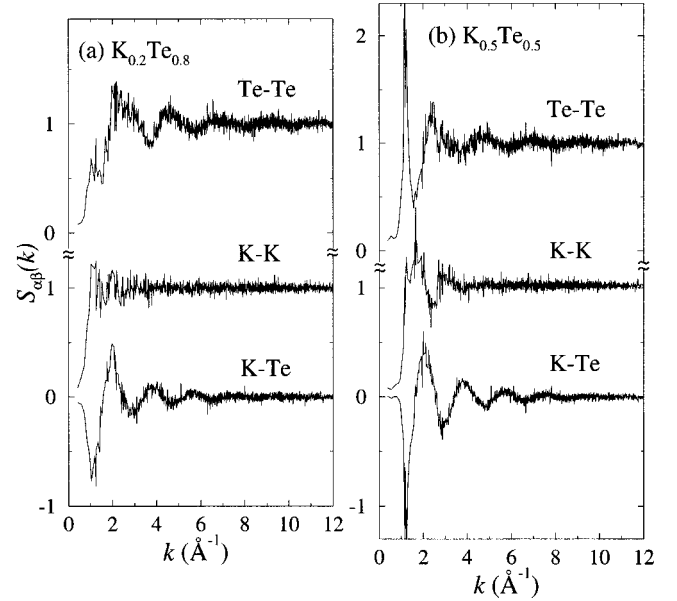


FIG. 1. The Ashcroft-Langreth partial structure factors $S_{\alpha\beta}(k)$ of the liquid (a) $K_{0.2}Te_{0.8}$ and (b) $K_{0.5}Te_{0.5}$.

at about $k = 2.1 \text{ \AA}^{-1}$, and an oscillating profile at larger $k > 3 \text{ \AA}^{-1}$. This behavior of the $S_{KTe}(k)$ becomes marked with increasing K concentration.

Before we investigate the dynamic properties of a Te chain structure in the liquid mixtures, it is important to confirm, by comparing calculated atomic structure with the experimental data, that our simulations are correctly carried out. We show in Fig. 2 the structure factors $S(k)$ for three K concentrations, $x = 0.0, 0.2,$ and 0.5 . The calculated $S(k)$ shown by the solid line is obtained from the partial structure factors with the neutron-scattering lengths ($b_{Te} = 5.43$ fm and $b_K = 3.7$ fm). The dashed and dotted lines show the results of neutron-diffraction measurements.^{4,6,28} We can see that the overall profile of the measured $S(k)$'s of the pure liquid Te and the liquid $K_{0.2}Te_{0.8}$ are reproduced fairly well by our simulation and that the calculated $S(k)$ of the liquid $K_{0.5}Te_{0.5}$ is in good agreement with the experiments. The first peak of the total $S(k)$ is originated from the corresponding peaks of the $S_{TeTe}(k)$ and $S_{KTe}(k)$. Up to $x = 0.2$, the oscillating profile for $k > 3 \text{ \AA}^{-1}$ is almost determined by the $S_{TeTe}(k)$, while at $x = 0.5$, it is dominated by the $S_{KTe}(k)$. It should be noted that the first sharp diffraction peak (FSDP) appears at $x = 0.5$, being in agreement with the experiment. In the case of the liquid Rb_xTe_{1-x} mixture,⁷ the FSDP was not observed even at $x = 0.5$, despite the fact that the $S_{\alpha\beta}(k)$'s are similar to those of the liquid K_xTe_{1-x} . This difference is simply caused by the fact that the neutron-scattering length of an Rb atom is larger than that of a K atom.

Figure 3 shows the partial pair distribution functions $g_{\alpha\beta}(r)$. The solid, dashed, and dotted lines show the $g_{TeTe}(r)$, $g_{KTe}(r)$, and $g_{KK}(r)$, respectively. From Fig. 3(a), we can see that there is no well-defined first coordination shell in the $g_{TeTe}(r)$ for the pure liquid Te. From Figs. 3(b) and 3(c), we see that the peaks of the $g_{TeTe}(r)$ and $g_{KTe}(r)$ become higher with increasing K concentration. The first

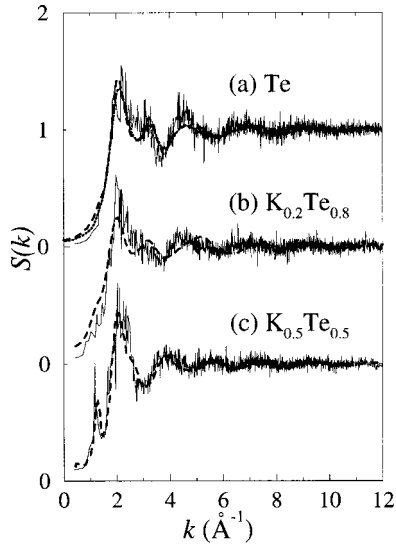


FIG. 2. The structure factors $S(k)$ of the liquid K_xTe_{1-x} for three K concentrations $x=(a)$ 0.0, (b) 0.2, and (c) 0.5. The calculated $S(k)$ shown by the solid line is obtained from the partial structure factors with the neutron-scattering lengths. The dashed and dotted lines show the results of neutron-diffraction measurements carried out by Kawakita *et al.* (Ref. 6) (dashed lines for pure liquid Te and liquid $K_{0.2}Te_{0.8}$), Takeda *et al.* (Ref. 28) (dotted line for pure liquid Te), and Fortner *et al.* (Ref. 4) (dashed line for liquid $K_{0.5}Te_{0.5}$).

minimum of the $g_{TeTe}(r)$ becomes deeper when the K concentration is increased. These facts indicate that the chain structure of Te is stabilized by the presence of K atoms. As for the $g_{KK}(r)$, it has broad distribution for both concentrations $x=0.2$ and 0.5, though a broad peak around 4.5 Å is recognized at $x=0.5$.

B. Electronic density of states

Figure 4 shows the concentration dependence of the electronic density of states (DOS) in the liquid K-Te mixtures, which is obtained from a time average of the distribution of the single-electron eigenvalues. The bold solid lines show the total DOS. The thin solid and thin dotted lines show the partial DOS for Te and K atoms, respectively. The partial DOS for α -type atom was obtained by projecting the wave functions on the spherical harmonics within a sphere of radius $S=1.1$ Å centered at each α -type atom.²⁹ The origin of the energy is taken to be the Fermi level ($E_F=0$). From Fig. 4(a), the DOS has large values around E_F , which means the metallic properties of the pure liquid Te is reproduced. As shown in Figs. 4(b) and 4(c), a dip at E_F in the total DOS arises from the presence of K atoms, and the dip becomes deeper with increasing K concentration, which is consistent with the observed concentration dependence of the electrical conductivity.⁶

The large peak at about -14 eV originates from the K 3p states. The Te 5s states are located between -13 and -9 eV, and the Te 5p states are located above -5 eV. At $x=0.5$, there are several sharp peaks in the partial DOS for Te; two peaks in the 5s states and three peaks in the 5p

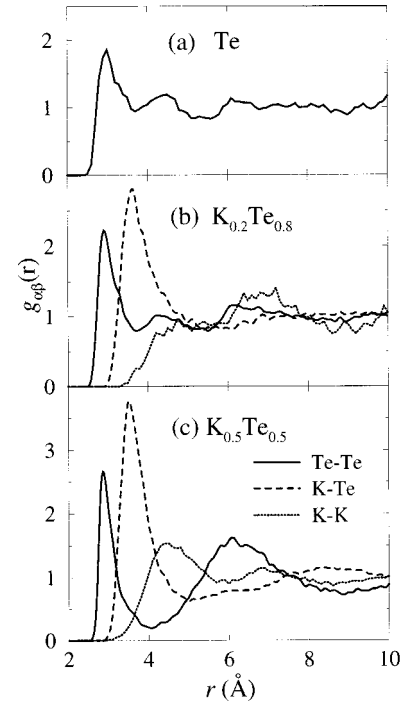


FIG. 3. The pair distribution functions $g_{\alpha\beta}(r)$ of the liquid K_xTe_{1-x} for three K concentrations $x=(a)$ 0.0, (b) 0.2, and (c) 0.5. The solid, dashed, and dotted lines show the $g_{TeTe}(r)$, $g_{KTe}(r)$, and $g_{KK}(r)$, respectively.

states below E_F correspond to the energy levels of the Te_2^{2-} dimer, which clearly indicates that the liquid mixture consists mainly of the Zintl anions at the equiatomic concentration. The partial DOS for K atoms has very small values

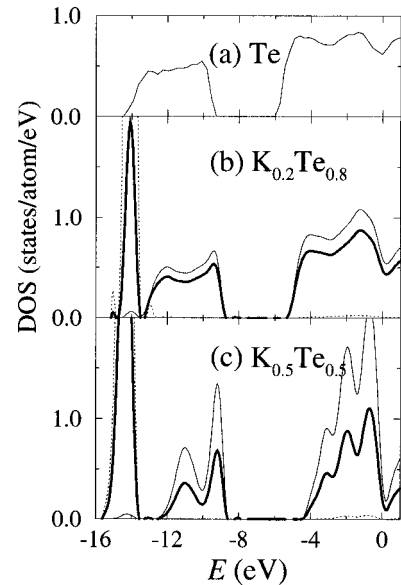


FIG. 4. The electronic density of states (DOS) of the liquid K_xTe_{1-x} for three K concentrations $x=(a)$ 0.0, (b) 0.2, and (c) 0.5. The bold solid lines show the total DOS. The thin solid and thin dotted lines show the partial DOS for Te and K atoms, respectively. The origin of the energy is taken to be the Fermi level ($E_F=0$).

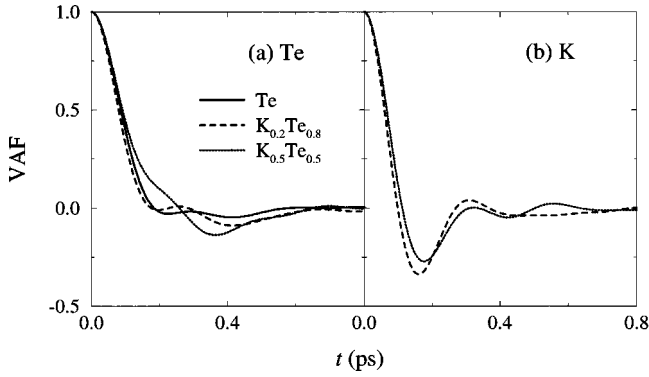


FIG. 5. The velocity autocorrelation functions (VAF) for (a) Te and (b) K atoms in the liquid K_xTe_{1-x} . The solid, dashed, and dotted lines show the VAF at $x=0.0, 0.2,$ and $0.5,$ respectively.

above -5 eV for both concentrations, which suggests that a nearly complete charge transfer from K to Te occurs, as was observed for the liquid Rb_xTe_{1-x} mixtures.⁷

C. Dynamic properties of atoms

To investigate the atomic dynamics in the liquid alkali tellurides, we have calculated the velocity autocorrelation functions (VAF), which are shown in Fig. 5. The solid, dashed, and dotted lines show the correlation functions at $x=0.0, 0.2,$ and $0.5,$ respectively. From Fig. 5(a), it is seen that the VAF for Te atoms in the liquid $K_{0.2}Te_{0.8}$ is similar to that in the pure liquid Te. On the other hand, the VAF for Te atoms at the equiatomic concentration is significantly different from the others; there appears the shoulder at about $t=0.25$ ps and the dip at about $t=0.38$ ps in the VAF for the liquid $K_{0.5}Te_{0.5}$. The Fourier transform of the VAF for Te atoms in these liquid mixtures consists of two broad peaks; the peaks at about 30 and 110 cm^{-1} are considered to be originated from the bending and stretching motion of Te atoms in the chain structure, respectively. In the liquid $K_{0.5}Te_{0.5}$, the frequency of the stretching motion is increased to about 150 cm^{-1} , which is due to the presence of the Te_2^{2-} dimers and is consistent with the appearance of the shoulder and dip at about $t=0.25$ and 0.38 ps, respectively, in the VAF. The VAF for K atoms in the liquid mixtures have an oscillating behavior as shown in Fig. 5(b), which is reflected by the cage effects.

D. Stability of chain structure

In order to investigate the stability of local chain structure formed by Te atoms in the liquid mixtures, we have analyzed (1) the three-dimensional atomic arrangements, (2) the distance $d_{ij}(t)$ between i th and j th Te atoms as a function of time t , and (3) the Te coordination number $n_i(t)$ of an i th Te atom. Not only by seeing the atomic arrangements but also by analyzing the $d_{ij}(t)$ and $n_i(t)$, will we be able to obtain highly detailed information about the time change of local atomic configurations.

Figure 6 shows the snapshots of the atomic configurations obtained by *ab initio* MD simulations. In the pure liquid Te [Fig. 6(a)] as many of the threefold coordinated Te atoms

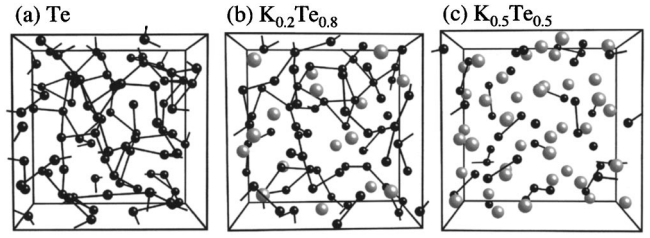


FIG. 6. The atomic configurations of the liquid K_xTe_{1-x} for three K concentrations $x=(a) 0.0,$ (b) $0.2,$ and (c) $0.5.$ The black and gray balls show the positions of Te and K atoms, respectively, in the supercell. Two Te atoms, whose distance apart is smaller than 3.25 Å, are connected by the bond.

exist as do the twofold coordinated ones, and the chain structure cannot be clearly seen. In the liquid $K_{0.2}Te_{0.8}$ [Fig. 6(b)], the number of the twofold coordinated Te atoms increases, and the chain structure can be recognized. We see from Fig. 6(b) that the Te chains are separated by the K atoms. At the equiatomic concentration [Fig. 6(c)], almost all Te atoms form Te_2 dimers. It should be noted that there exists short Te chains, which consist of more than two Te atoms, and isolated Te atoms.

Figure 7 displays some examples of the time evolution of the distance $d_{ij}(t)$, where the $d_{ij}(t)$ between a focused (i th) Te atom selected arbitrarily and all other (j th) Te atoms are shown for three K concentrations. From the $d_{ij}(t)$'s in the pure liquid Te, we see that the distances between two Te atoms change largely with time, and that each Te atom is almost always surrounded by more than one Te atom. We can recognize the stretching motion between pairs of Te atoms [oscillation of $d_{ij}(t)$ around 3 Å with small ampli-

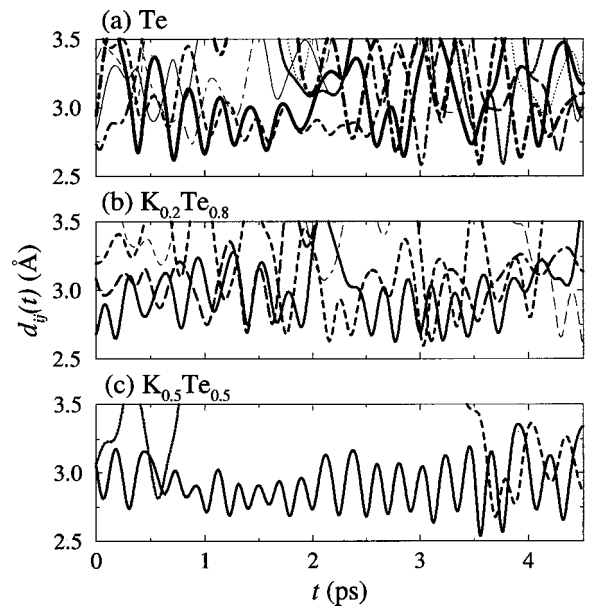


FIG. 7. The time evolution of the distance $d_{ij}(t)$ between i th and j th Te atoms in the liquid K_xTe_{1-x} for three K concentrations $x=(a) 0.0,$ (b) $0.2,$ and (c) $0.5.$ Each figure shows the distance $d_{ij}(t)$ between a focused (i th) Te atom selected arbitrarily and all other (j th) Te atoms.

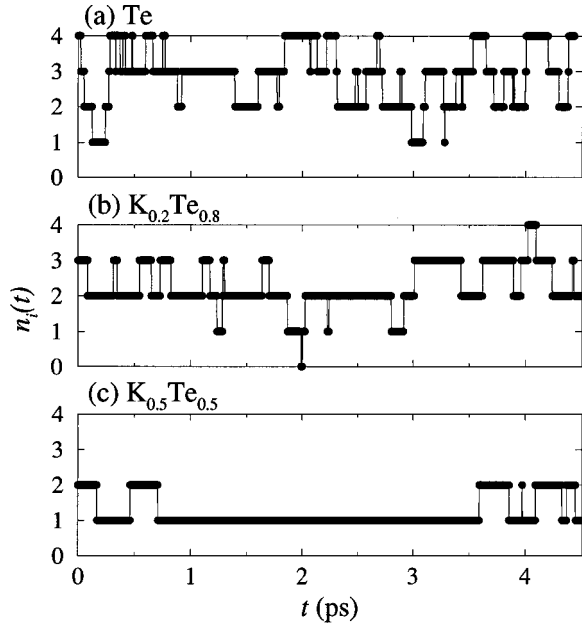


FIG. 8. The time evolution of the coordination number $n_i(t)$ of i th Te atoms in the liquid $K_x\text{Te}_{1-x}$ for three K concentrations x = (a) 0.0, (b) 0.2, and (c) 0.5.

tudes] being reflected by a covalent bonding. We see, however, that such vibrating motion does not continue for longer than 2 ps, and that each Te atom switches its neighbors (the bond switching) frequently; we can see that a distance $d_{ij}(t)$ increases suddenly, and instead the other distance $d_{ij'}(t)$ decreases at the same time [see Fig. 7(a)].

Similar to the pure liquid Te, the $d_{ij}(t)$'s change largely with time in the liquid $K_{0.2}\text{Te}_{0.8}$. It is, however, seen that when compared with the pure liquid Te, (i) the number of lines shown in the figure [Fig. 7(b)] decreases, (ii) the stretching motion appears more clearly, and (iii) the bond switching occurs less frequently.

In the liquid $K_{0.5}\text{Te}_{0.5}$, the time evolution of the $d_{ij}(t)$'s is completely different from those in the other liquids; (i) only a few lines are shown in the figure [Fig. 7(c)], (ii) the stretching motion appears clearly and continues for a relatively long time, and (iii) the bond switching occurs only rarely. We see from Fig. 7 that the frequency of the stretching motion at the equiatomic concentration is higher than those in the other liquids, which is consistent with the values obtained by the VAF.

The Te atom has the twofold coordination in a chain structure, while it has the onefold coordination if the Zintl Te_2^{2-} anion is formed. Therefore, by investigating the coordination number $n_i(t)$ of i th Te atoms as a function of time t , we will be able to obtain the information about the time change of local atomic configurations in more detail. We have calculated the $n_i(t)$ by counting the number of Te atoms, which are within a distance of $R=3.25$ Å from the i th Te atom, at a time t . Figure 8 displays some examples of the $n_i(t)$ for three K concentrations. Note that the $n_i(t)$ depends somewhat on the value of R , but the following qualitative features of $n_i(t)$ would not depend on the choice of R .

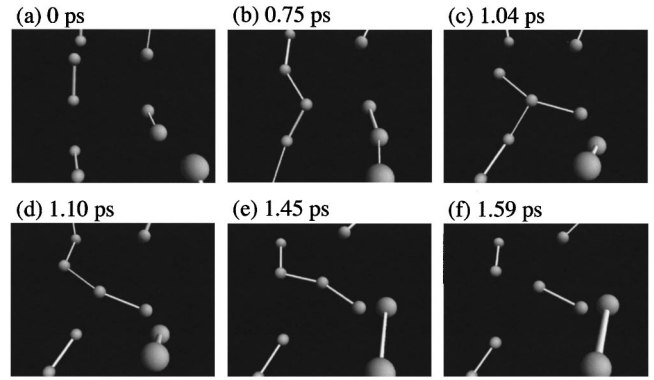


FIG. 9. The time evolution of local atomic configurations in the liquid $K_{0.5}\text{Te}_{0.5}$. The balls show the positions of Te atoms. The positions of K atoms are not shown. Two Te atoms, whose distance apart is smaller than 3.25 Å, are connected by the bond.

Comparing the results for the pure liquid Te with those for the liquid $K_{0.2}\text{Te}_{0.8}$, we see that in the liquid $K_{0.2}\text{Te}_{0.8}$, Te atoms have the twofold coordination for a longer time and change the value of $n_i(t)$ less frequently. (Taking the average, Te atoms change the value of $n_i(t)$ about 50 times for 4.5 ps in the liquid Te, while about 40 times in the liquid $K_{0.2}\text{Te}_{0.8}$.) These features clearly show that the chain structure is stabilized by the presence of K atoms.

It is seen that in the three liquids, Te atoms have the onefold coordination for the longest time in the liquid $K_{0.5}\text{Te}_{0.5}$, although they have also the twofold coordination at irregular intervals. We conclude that the *most stable* structure is formed at the equiatomic concentration [in the sense that Te atoms change the value of $n_i(t)$ less than 20 times on average for 4.5 ps], although the structure does depend on the time.

As stated in the previous subsection, the partial DOS for Te atoms (Fig. 4) clearly indicates that the liquid mixture consists mainly of the Te_2^{2-} dimers at the equiatomic concentration. This was confirmed by seeing the spatial configuration of atoms [Fig. 6(c)]. These results are quite consistent with the expectation of the Zintl rule.^{10,11} However, the time evolution of the $n_i(t)$ (Fig. 8) seems to be inconsistent with this expectation. If all Te atoms formed the Te_2^{2-} dimers, the $n_i(t)$ would be one and would not change with time. To solve this puzzle, we have to see the time change of local atomic configurations directly as shown in Fig. 9, where the balls show the positions of Te atoms. Two Te atoms, whose distance apart is smaller than 3.25 Å, are connected by the bond. In Fig. 9(a), several dimers are shown. After 0.75 ps [Fig. 9(b)], chain structures appear by connecting dimers. At 1.04 ps [Fig. 9(c)], a bond in the right chain is broken, and a new bond is formed between the Te atom, which belonged to the right chain, and one of Te atoms in the left chain. We can see the Te atom in the left chain has the threefold coordination. As displayed in Fig. 9(d), one of the bonds associated with the threefold coordinated Te atom is broken at 1.10 ps. Although a short chain containing four Te atoms exists for a while [Fig. 9(e)], it is broken into two dimers as shown in Fig. 9(f). Finally, a local atomic configuration consisting of dimers is obtained.

In conclusion, it is certain that the liquid K-Te mixture consists mainly of the Te_2^{2-} dimers at the equiatomic concentration as expected by the Zintl rule. However, it is not correct to consider that the Te_2^{2-} dimers exist *stably* in the same way as a neutral Te_2 dimer exists in a vacuum. In fact, since two *extra* electrons in a Te_2^{2-} dimer occupy the antibonding π states, the covalent bond in the Te_2^{2-} dimer must be weaker than that in the neutral Te_2 dimer. As shown in Fig. 9, in the liquid $\text{K}_{0.5}\text{Te}_{0.5}$ mixture, the Zintl Te_2^{2-} dimers interact with each other, and the bond breaking and the rearrangement of dimers occur rather frequently.

IV. SUMMARY

The stability of local chain structures formed by Te atoms, as well as the atomic structure and the electronic density of states in liquid $\text{K}_x\text{Te}_{1-x}$ mixtures with $x=0.0, 0.2,$ and 0.5 have been investigated by *ab initio* molecular-dynamics (MD) simulations. It is shown that the calculated structure factors are in good agreement with the experimental results in a wide range of K concentration, and that the transition from the metallic to the semiconducting states with increasing alkali elements is well reproduced by our *ab initio* MD simulations. By investigating the distances between two Te atoms and the coordination number of each Te atom as a

function of time, it is seen that with increasing K concentration, the stretching motion of Te atoms appears more clearly and continues for a longer time, and the bond switching in the chain structure occurs less frequently, which means the chain structure is more stabilized by the presence of K atoms. The partial electronic density of states and the spatial atomic configuration show that at the equiatomic concentration, most of the Te atoms form the Te_2^{2-} anions, as expected by the Zintl rule. It is, however, found from the detailed analysis of the time evolution of local atomic structures that the Zintl Te_2^{2-} anions interact with each other, and the bond breaking and the rearrangement of dimers occur rather frequently in the liquid $\text{K}_{0.5}\text{Te}_{0.5}$ mixture.

ACKNOWLEDGMENTS

We would like to thank Dr. Y. Kawakita, Professor M. Yao, and Professor S. Takeda for providing us with their experimental data. This work was supported by a Grant-in-Aid for Scientific Research from The Ministry of Education, Science, Sports, and Culture, Japan. We are grateful to the Supercomputer Center, Institute for Solid State Physics, University of Tokyo for the use of SGI 2800 and Hitachi SR8000 supercomputers.

-
- ¹C. A. Kraus and S. W. Glass, *J. Phys. Chem.* **33**, 984 (1929).
²M.-L. Saboungi, J. Fortner, J. W. Richardson, A. Petric, M. Doyle, and J. E. Enderby, *J. Non-Cryst. Solids* **156-158**, 356 (1993).
³Y. Kawakita, M. Yao, H. Endo, and J. Dong, *J. Non-Cryst. Solids* **205-207**, 447 (1996).
⁴J. Fortner, M.-L. Saboungi, and J. E. Enderby, *Phys. Rev. Lett.* **69**, 1415 (1992).
⁵Y. Kawakita, J. Dong, T. Tsuzuki, Y. Ohmasa, M. Yao, H. Endo, H. Hoshino, and M. Inui, *J. Non-Cryst. Solids* **156-158**, 756 (1993).
⁶Y. Kawakita, M. Yao, and H. Endo, *J. Phys. Soc. Jpn.* **66**, 1339 (1997).
⁷F. Shimojo, K. Hoshino, and Y. Zempo, *Phys. Rev. B* **59**, 3514 (1999).
⁸J. Hafner, K. Seifert-Lorentz, and O. Genser, *J. Non-Cryst. Solids* **250-252**, 225 (1999).
⁹J. Getzschmann, P. Böttcher, and W. Kaluza, *Z. Kristallogr.* **211**, 90 (1996).
¹⁰E. Zintl, J. Goubeau, and W. Dullenkopf, *Z. Phys. Chem. Abt. A* **154**, 1 (1931).
¹¹W. van der Lugt, *J. Phys.: Condens. Matter* **8**, 6115 (1996).
¹²G. Galli and M. Parrinello, *J. Chem. Phys.* **95**, 7504 (1991).
¹³M. Schöne, R. Kaschner, and G. Seifert, *J. Phys. Condens. Matter* **7**, L19 (1995).
¹⁴Y. Senda, F. Shimojo, and K. Hoshino, *J. Phys.: Condens. Matter* **12**, 6101 (2000).
¹⁵Y. Senda, F. Shimojo, and K. Hoshino, *J. Phys.: Condens. Matter* **11**, 2199 (1999).
¹⁶Y. Senda, F. Shimojo, and K. Hoshino, *J. Phys.: Condens. Matter* **11**, 5387 (1999).
¹⁷G. A. de Wijs, G. Pastore, A. Selloni, and W. van der Lugt, *J. Chem. Phys.* **103**, 5031 (1995).
¹⁸K. Seifert-Lorentz and J. Hafner, *Phys. Rev. B* **59**, 843 (1999).
¹⁹J. P. Perdew, K. Burke, and M. Ernzerhof, *Phys. Rev. Lett.* **77**, 3865 (1996).
²⁰T. A. Arias, M. C. Payne, and J. D. Joannopoulos, *Phys. Rev. B* **45**, 1538 (1992).
²¹G. Kresse and J. Hafner, *Phys. Rev. B* **49**, 14 251 (1994).
²²F. Shimojo, Y. Zempo, K. Hoshino, and M. Watabe, *Phys. Rev. B* **52**, 9320 (1995).
²³D. Vanderbilt, *Phys. Rev. B* **41**, 7892 (1990).
²⁴G. Kresse and J. Hafner, *J. Phys.: Condens. Matter* **6**, 8245 (1994).
²⁵S. Nosé, *Mol. Phys.* **52**, 255 (1984).
²⁶W. G. Hoover, *Phys. Rev. A* **31**, 1695 (1985).
²⁷N. W. Ashcroft and D. C. Langreth, *Phys. Rev.* **159**, 500 (1967).
²⁸S. Takeda, S. Tamaki, and Y. Waseda, *J. Phys. Soc. Jpn.* **53**, 3830 (1984).
²⁹F. Shimojo, S. Munejiri, K. Hoshino, and Y. Zempo, *J. Phys.: Condens. Matter* **11**, L153 (1999).